SMAALEN, S. VAN (1991*c*). *Methods of Structure Analysis of Modulated Structures and Quasicrystals*, edited by J. M. PÉREZ-MATO, F. J. ZUNIGA, G. MADARIAGA & A. LOPEZ-ECHARRI, pp. 90–106. Singapore: World Scientific.
SMAALEN, S. VAN (1992). *Mater. Sci. Forum*, **100&101**, 173–222.
SMAALEN, S. VAN, MEESTMA, A., WIEGERS, G. A. & DE BOER, J. L. (1991). *Acta Cryst.* B**47**, 314–325.
SMAALEN, S. VAN & PETŘÍČEK, V. (1992). *Acta Cryst.* A**48**, 610–618.
UKEI, K., YAMAMOTO, A., WATANABE, Y., SHISHIDO, T. & FUKUDA, T. (1992). *Acta Cryst.* B**49**, 67–72.
WALKER, M. B. & QUE, W. (1992). *Phys. Rev. B*, **45**, 8085–8090.
WANG, S. & KUO, K. H. (1991). *Acta Cryst.* A**47** 381–392.
WIEGERS, G. A. & MEERSCHAUT, A. (1992). *J. Alloys Comp.* **173**, 351–368.
WIEGERS, G. A., MEETSMA, A., DE BOER, J. L., VAN SMAALEN, S. & HAANGE, R. J. (1991). *J. Phys. Condens Mat.* **3**, 2603–2612.
WIEGERS, G. A., MEETSMA, A., HAANGE, R. J. & DE BOER, J. L. (1989). *Solid State Ionics*, **32/33**, 183–191.
WIEGERS, G. A., MEETSMA, A., HAANGE, R. J. & DE BOER, J. L. (1990). *J. Solid State Chem.* **89**, 328–339.
WIEGERS, G. A., MEETSMA, A., HAANGE, R. J. & DE BOER, J. L. (1991). *J. Less-Common. Met.* **3**, 2603–2612.
WIEGERS, G. A., MEETSMA, A., HAANGE, R. J., VAN SMAALEN, S., DE BOER, J. L., MEERSCHAUT, A., RABU, P. & ROUXEL, J. (1990). *Acta Cryst.* B**46**, 324–332.
WIEGERS, G. A., MEETSMA, A., VAN SMAALEN, S., HAANGE, R. J. & DE BOER, J. L. (1990). *Solid State Commun.* **75**, 689–692.
WILLIAMS, T. B. & HYDE, B. G. (1988). *Phys. Chem. Miner.* **15**, 521–544.
WOLFF, P. M. DE (1974). *Acta Cryst.* A**30**, 777–785.
WOLFF, P. M. DE, JANSSEN, T. & JANNER, A. (1981). *Acta Cryst.* A**37**, 625–636.
WULFF, J., MEETSMA, A., HAANGE, R. J., DE BOER, J. L. & WIEGERS, G. A. (1990). *Synth. Met.* **39**, 1–12.
WULFF, J., MEETSMA, A., VAN SMAALEN, S., HAANGE, R. J., DE BOER, J. L. & WIEGERS, G. A. (1990). *J. Solid State Chem.* **84**, 118–129.
YAMAMOTO, A. (1982*a*). *Acta Cryst.* A**38**, 87–92.
YAMAMOTO, A. (1982*b*). *Acta Cryst.* B**38**, 1446–1451.
YAMAMOTO, A. (1982*c*). *Acta Cryst.* B**38**, 1451–1456.
YAMAMOTO, A. (1992). *Acta Cryst.* A**48**, 476–483.
YAMAMOTO, A., JANSSEN, T., JANNER, A. & DE WOLFF, P. M. (1985). *Acta Cryst.* A**41**, 528–530.
YAMAMOTO, A. & NAKAZAWA, H. (1982). *Acta Cryst.* B**38**, 79–86.
YAMAMOTO, A., NAKAZAWA, H., KITAMURA, M. & MORIMOTO, N. (1984). *Acta Cryst.* B**40**, 228–237.
YAMAMOTO, A., ONODA, M., TAKAYAMA-MUROMACHI, E., IZUMI, F., ISHIGAKI, T. & ASANO, H. (1990). *Phys. Rev. B*, **42**, 4228.
YAMAMOTO, A., TAKAYAMA-MUROMACHI, E., IZUMI, F., ISHIGAKI, T. & ASANO, H. (1993). *Physica (Utrecht)*. In the press.
ZHOU, W. Y., MEETSMA, A., DE BOER, J. L. & WIEGERS, G. A. (1992). *Mater Res. Bull.* **27**, 563–572.

Acta Cryst. (1993). A**49**, 846–853

Approximate Model for the Crystal Structure of Precipitates in NaF Doped with AlF_3

BY KAZUO SUZUKI*

Hokkaido Tokai University, Sapporo, Hokkaido, Japan

(*Received* 12 *October* 1992; *accepted* 4 *May* 1993)

Abstract

The crystal structure of precipitates in a mixed crystal of NaF and 1 mol% AlF_3 has been studied at room temperature using both stationary-crystal and rotating-crystal X-ray photographic methods. It has been found that almost all the reflections can be assigned to a face-centered-cubic (f.c.c.) lattice with unit-cell parameter 7.77 Å. The main feature of the diffraction pattern is that the 311 reflection is very strong while the 222 reflection is practically zero, in contrast to the case of high-form cryolite, *i.e.* cubic Na_3AlF_6. These features are explained by assuming an f.c.c. arrangement of AlF_6 octahedra that are rotated around the ⟨111⟩ axes by about 47° from the highest-symmetry orientation. It has also been shown that the F ions in each octahedron make large overlaps with the Al ion at the center of the octahedron. A random distribution of rotation axes is also proposed to conform to the cubic symmetry of the lattice structure of the precipitate.

1. Introduction

In several previous papers concerning mixed crystals of alkali halides doped with divalent cations, we have reported segregation of some kinds of metastable centers (Miyake & Suzuki, 1954*a*,*b*; Suzuki, 1955, 1958, 1961). As an extension of these investigations, it seems interesting to try to use trivalent cations for impurity doping. When a trivalent cation replaces a monovalent cation constituting a matrix lattice, it is accompanied by two cation vacancies and several types of dipole interactions may be expected.

A study of NaF doped with AlF_3 was tried because: (i) according to the phase diagram shown in Fig. 1 (Fedotieff & Iljinskii, 1913),† this system is

* A part of this work was done when the author was at the Muroran Institute of Technology, Muroran, Hokkaido, Japan.

† We have referred to this phase diagram, which is published in *Phase Diagrams for Ceramists*, 4th printing, 1979, The American Ceramic Society, Ohio, USA.

©1993 International Union of Crystallography
Printed in Great Britain – all rights reserved

ISSN 0108-7673 ©1993

expected to exhibit a high degree of solid solubility at concentrations of a few mol% AlF_3; (ii) AlF_3 is relatively stable at high temperatures so that AlF_3 doping is expected to be easy. However, X-ray diffraction photographs for the as-grown crystal indicated precipitates that were incoherent to the matrix. The diffraction patterns of the precipitates show interesting features as follows: (i) stationary-crystal photographs show that distribution of the diffraction spots of the precipitates has the same symmetry as that of the matrix lattice; (ii) a rotating-crystal photograph reveals diffraction lines due to the precipitates and almost all of the lines can be indexed with f.c.c. indices.

Several kinds of growing conditions were tried in order to grow mixed crystals with homogeneous solid solutions in this system. The results were not, however, what was expected. As-grown crystals were then reheated in nitrogen gas at higher temperatures, for example at 1173 K for 0.5 h, and were quenched to room temperature. As a result, the groups of spots of the precipitates on the stationary-crystal photographs changed to continuous lines but did not disappear. We conclude that, contrary to the phase diagram, the precipitated phase is stable up to 1173 K. We have not studied the incipient precipitation for this system.

The present paper reports X-ray observations of the precipitates by the rotating-crystal photographic method and proposes an appropriate model for the crystal structure of the precipitate. Although the model is not complete, it is conceived to be an essential one for explaining the diffraction intensities of the precipitate.

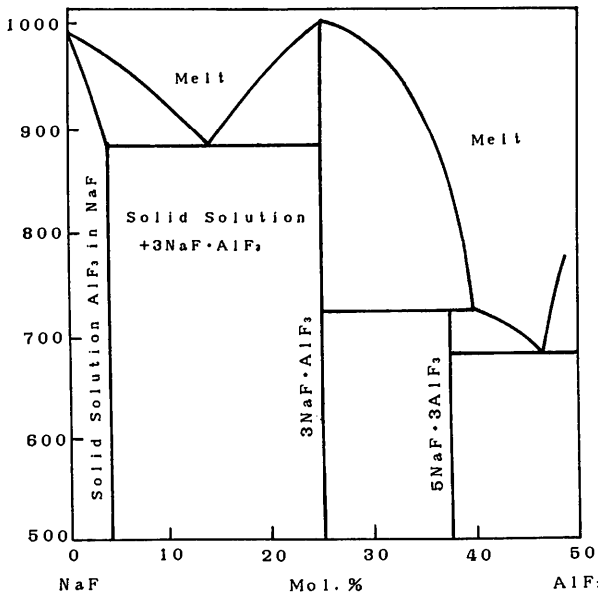

Fig. 1. Phase diagram for the system NaF–AlF_3 (Fedotieff & Iljinskii, 1913).

2. Preparation of samples

Single crystals of NaF doped with 1 mol% AlF_3 were prepared by the Bridgman method. An SiC ribbon heater, 'Siliconit', of the double-spiral type, was used as a cylindrical electric furnace. A graphite crucible was supported in the furnace by a stainless-steel rod, which allowed the crucible to move vertically along the central axis of the furnace. The rod was driven by a stepping motor. The air in the furnace tube was replaced by nitrogen gas, which flowed very slowly. The flow rate of the gas was monitored roughly by a water bubbler.

The pulverized mixture of NaF and AlF_3 that filled the crucible was melted by being maintained at 1373 K for 1 h. The melt was then solidified from the bottom by moving the crucible down to low-temperature regions in the furnace at the rate 4.4 mm h^{-1}. After that, the furnace temperature was lowered at the maximum rate of ~ 100 K h^{-1}. The transparency of the crystal block thus grown was not uniform but consisted of a fairly transparent zone in the lower part and a cloudy zone in the upper part of the block. The samples used for the X-ray examination were cut out of the relatively transparent zone. As-grown crystals were used for the samples.

3. X-ray observation

X-ray photographs were taken with the crystal at room temperature, using monochromatic Cu $K\alpha$ radiation reflected by a pyrolytic graphite monochromator. A cylindrical camera with radius 35.0 mm was used.

Two stationary-crystal photographs are shown in Fig. 2. The [001] axis of the matrix was kept vertical. In the case of Fig. 2(*a*), the incident beam is parallel to the [010] direction; in the case of Fig. 2(*b*), it is parallel to the [110] direction. Relatively weak diffraction from the precipitates is observed, superposed on very strong reflections from the matrix. The patterns of the precipitates are very spotty, with some preferred orientation, and are symmetric, with {100} and {110} mirror planes. Asymmetry in the intensities in Fig. 2(*b*) is due to absorption by the specimen.

Fig. 3. shows a rotating-crystal photograph around the [001] axis of the matrix. In this photograph, the pattern is composed of three kinds of reflections: (i) Very strong NaF-matrix reflections lying on layer lines. (ii) Reflection spots of medium or weak intensity, some on the matrix layer lines and others at intermediate positions. All these spotty reflections are explicable as NaF-matrix reflections of

second- or third-order Cu radiation with wavelength $\lambda/2$ or $\lambda/3$ from the monochromator. (iii) Weak Debye–Scherrer lines from the precipitates, some rather continuous and others somewhat fragmentary, owing to the limited distribution of orientations (preferred orientation) of the precipitates. However, the intensity variation on each line is not large, so that visual estimations of relative intensities of the reflections are possible. Structure analysis of the precipitate has been performed on the basis of these Debye–Scherrer lines.

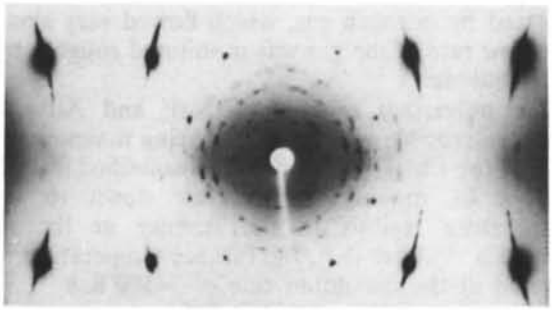

(*a*)

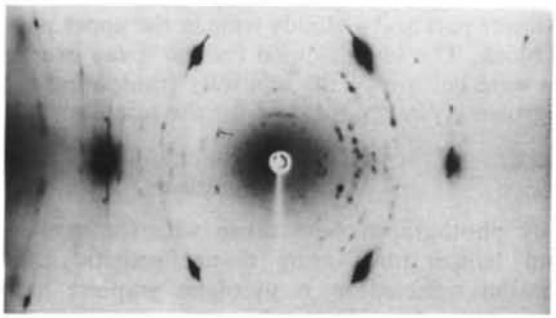

(*b*)

Fig. 2. Stationary-crystal X-ray photographs of NaF + 1 mol% AlF_3. The [001] axis of the matrix is vertical. Cu $K\alpha$ radiation reflected by a pyrolytic graphite monochromator. Cylindrical camera. (*a*) Incident beam parallel to the [010] lirection. (*b*) Incident beam parallel to the [110] direction.

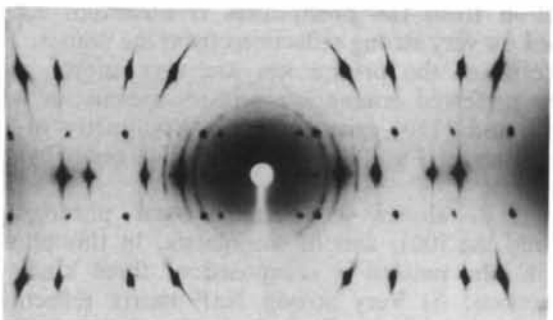

Fig. 3. Rotating-crystal X-ray photograph of NaF + 1 mol% AlF_3. Rotation around the [001] axis of the matrix. Cu $K\alpha$ radiation reflected by a pyrolytic graphite monochromator. Cylindrical camera.

Table 1. *Lattice spacings and indices for diffraction lines of the precipitate*

Reflections with indices in parentheses are forbidden to f.c.c. and are omitted in the calculation of the mean value of the lattice constant.

θ (rad)	d (Å)	hkl	a (Å)	$\Delta a/a_0$ (%)
0.17122	4.5244	111	7.836	+0.89
0.19928	3.8941	200	7.788	+0.27
0.22662	3.4310	(210)	7.672	−1.22
0.28417	2.7497	220	7.777	+0.13
0.33813	2.3239	311	7.708	−0.76
0.37050	2.1291	(230)	7.676	−1.17
0.40647	1.9498	400	7.799	+0.41
0.46043	1.7350	420	7.759	−0.10
0.51079	1.5769	422	7.725	−0.54
0.54317	1.4915	333,511	7.750	−0.22
0.59353	1.3784	440	7.797	+0.39
0.62950	1.3094	531	7.747	−0.26
0.67986	1.2262	620	7.755	−0.15
			a_0 (mean value) = 7.77 Å	

3.1. *Lattice parameter and unit-cell volume of the precipitate*

Lattice spacings estimated from the diffraction lines are listed in Table 1. Almost all the lines, with the exception of the 210 and 230 lines, are assigned by f.c.c. indices. The 210 line is ignored in the subsequent structure analysis because of its extremely weak intensity. Although the 230 line has considerable intensity, it also was not taken into account. A brief comment is given in § 5 on the possible origins of these reflections. The lattice parameter evaluated from each line is distributed in the range 7.73–7.84 Å, of which the average is taken to be 7.77 Å. The volume of the unit cell is 469.1 $Å^3$.

Cryolite, Na_3AlF_6, has monoclinic symmetry, with space group $P2_1/n$–C_{2h}^5 at ordinary temperatures. Its bimolecular cell has the dimensions $a_0 = 5.46$, $b_0 = 5.61$, $c_0 = 7.80$ Å, $\beta = 90° 11'$ (Naray-Szabo & Sasvari, 1938). At 823 K, it becomes cubic with space group $Fm\bar{3}m$–O_h^5 and the lattice parameter $a_0 = 7.95$ Å (Steward & Rooksby, 1953). The former is referred to hereinafter as cryolite and the latter as cubic Na_3AlF_6.

In the case of the cryolite, two translation vectors with magnitudes $a_0' = b_0' = (a_0^2 + b_0^2)^{1/2} = 7.83$ Å in the (001) plane of the monoclinic cell and a third vector of magnitude $c_0' = c_0 = 7.80$ Å constitute a pseudocubic double cell. This pseudocubic cell is directly related to the unit cell of cubic Na_3AlF_6, in that the former can be obtained from the latter by slight deformation. The volume of the pseudocubic cell of cryolite is 477.8 $Å^3$, coinciding with that of the precipitate within experimental error. Better agreement can be obtained by a comparison with recent data for cryolite listed in Powder Diffraction File No. 25-772 (JCPDS-ICDD, Pennsylvania, USA): $a_0 = 7.769$, $b_0 = 5.593$, $c_0 = 5.404$ Å, $\beta = 90.18°$. From these values, the volume of the pseudocubic cell is estimated to be 469.6 $Å^3$.

Table 2. *Relative intensities of diffraction by the precipitate and by cubic* Na_3AlF_6

		Cubic Na_3AlF_6	
hkl	Precipitate	Majumdar & Roy (1965)	Steward & Rooksby (1953)
111	*s*	50	*s*
200	*s*	50	*s*
(210)	*vvw*	–	–
220	*vs*	70	*vs*
311	*vs*	–	(NaF)
222	–	70	*s*
(230)	*w*	–	–
400	*vs*	100	*vs*
331	–	–	–
420	*w*	25	*w*
422	*s*	–	*s*
333,511	*vw*	–	*w*
440	*w*	15	*m*
531	*vw*	10	*vw*
600,4420	–	–	*vw*
620	*w*	–	*w*

3.2. *Intensities of diffraction lines*

Visual estimates of relative intensities of the diffraction lines of the precipitates are shown in Table 2, together with relative intensities for cubic Na_3AlF_6 given by Majumdar & Roy (1965)* and the visual estimate made by the present author for the diffraction lines seen on the photograph presented by Steward & Rooksby (1953).

Comparison of the intensities of the precipitates with those of cubic Na_3AlF_6 reveals the following characteristics: (i) in the case of the precipitate, the 222 reflection is practically zero while the 311 reflection is very strong; (ii) in the case of cubic Na_3AlF_6, the 222 reflection is strong while the 311 reflection is not recorded in the data of Majumdar & Roy (1965). In the photograph of Steward & Rooksby (1953), an NaF line is superposed on the 311 line of cubic Na_3AlF_6. On the other hand, in the case of the precipitate, only a small part of the 311 line overlaps the NaF reflection so visual estimation of the 311 reflection is possible.

4. Approximate model for the crystal structure of the precipitate

The overall features of the relative intensities of the diffractions of the precipitate are very similar to those of cubic Na_3AlF_6, except for 311 and 222. It is conceivable, therefore that the structure of the precipitate is closely related to that of cubic Na_3AlF_6.

4.1. AlF_6 *octahedra in the highest-symmetry orientation*

The crystal structure of cubic Na_3AlF_6 has been described by Steward & Rooksby (1953). We often refer to smaller cubic cells, making up the 'sublattice', that have edge lengths half those of the original cubic cells. The basic feature of the structure is the f.c.c. arrangment of AlF_6 octahedra with four Na ions forming links between the F ions and another eight Na ions filling certain gaps in the unit cell. Hereafter, the latter Na ions are tentatively assumed to be at body centers of the sublattice. However, the orientations of the octahedra relative to the axes of the unit cell are not known.

On the basis of the similarities between the precipitate and cubic Na_3AlF_6 described in the preceding section, the AlF_6 octahedra and Na ions of the precipitate are assumed to be at the following special positions of $Fm\bar{3}m$:

AlF_6: 000; f.c.,

Na: 1/2 1/2 1/2; f.c.;

$\pm$(1/4 1/4 1/4; 1/4 1/4 −1/4; −1/4 1/4 1/4;
1/4 −1/4 1/4).

Then, the structure factor of the unit cell is given by

$$\begin{aligned} F(hkl) = f_{AlF_6}[&1+\exp\pi i(h+k)+\exp\pi i(k+l)\\ &+\exp\pi i(l+h)]\\ &+f_{Na}[\exp\pi ih+\exp\pi ik+\exp\pi il\\ &+\exp\pi i(h+k+l)+2\cos\pi(h+k+l)/2\\ &+2\cos\pi(h+k-l)/2\\ &+2\cos\pi(-h+k+l)/2\\ &+2\cos\pi(h-k+l)/2], \end{aligned} \quad (1)$$

where f_{Na} is the atomic scattering factor of the Na ion. When the AlF_6 octahedron at 0,0,0 of the unit cell is in the highest-symmetry orientation, the Al and F ions are at

Al: 000,

F: $\pm(s00; 0s0; 00s)$,

where $s = 1/4 - u$ and u is a parameter representing the distance of an F ion from the nearest neighboring midpoint between Al and Na ions. Then, the structure factor of the AlF_6 octahedron is

$$f_{AlF_6} = f_{Al} + 2f_F(\cos 2\pi sh + \cos 2\pi sk + \cos 2\pi sl), \quad (2)$$

where f_{Al} and f_F are the atomic scattering factors of the Al and F ions.

The relative intensities of diffraction are calculated from

$$I = I(0)|F(hkl)|^2 nLpD, \quad (3)$$

where $I(0) = (I_e/p)(\lambda^3/v_c^2)$. I_e is the intensity of scattering by one electron, p is the polarization factor, v_c is the volume of the crystal taking part in the diffraction, n is the multiplicity, L is the Lorentz factor and D is the temperature factor. The diffraction pattern

* The data of Majumdar & Roy appeared as Powder Diffraction File No. 18-1214 at the JCPDS.

Table 3. *I/I(0) for the 311 and 222 reflections normalized by the 400 reflection when the AlF_6 octahedra are in the highest-symmetry orientation*

hkl	(i) $u = 1/63$	(ii) $u = 1/32$	(iii) $u = 1/21$
311	0.04	0.3	0.6
222	63	60	54
400	100	100	100

of the rotating-crystal photograph for the precipitate is regarded as continuous rings and the following formula is applied for the Lorentz–polarization factors:

$$\mathrm{Lp} = (1/\sin^2\theta\cos\theta)[(1+\cos^2 2\alpha\cos^2 2\theta)/(1+\cos^2 2\alpha)]$$
$$= (1+0.8\cos^2 2\theta)/1.8\sin^2\theta\cos\theta,$$

where α, the angle of reflection from the monochromator, is 13.28°. The temperature factor is

$$D = \exp(-16\pi^2\delta^2\sin^2\theta/3\lambda^2),$$

where δ^2 is the mean-square displacement of the ion, which is assumed to be 0.04 Å^2.

$I/I(0)$ is evaluated for the following three cases: (i) F ions make contacts with neighboring Al ions. In this case, $sa_0 = 1.82$ Å, $u = 1/63$; (ii) F ions make overlaps with both Al and Na ions to the same extent. In this case, $sa_0 = 1.70$ Å, $u = 1/32$; (iii) F ions make contacts with neighboring Na ions. In this case, $sa_0 = 1.58$ Å, $u = 1/21$. (i) and (iii) correspond to extreme positions of F ions and (ii) corresponds to the intermediate position. In the evaluation of ionic positions, the following values of ionic radii are used (Huheey, 1983): Na 1.16 Å, F 1.145 Å, Al 0.675 Å.

Table 3 shows normalized values of $I/I(0)$ for the 311 and 222 reflections for the three cases (i), (ii) and (iii). It is seen that, for (iii), the 311 reflection is a little larger and the 222 reflection is a little smaller compared with the other two cases. However, all of them are very different from the observation.

4.2. *Rotation of AlF_6 octahedra*

We have examined a number of modifications for the structure on the basis of the cubic Na_3AlF_6 structure, especially by taking into account the reversal of intensities between the 311 and the 222 lines. Steward & Rooksby (1953) pointed out that the positions of F ions in the monoclinic cell of cryolite could be represented by rotation or displacement of AlF_6 octahedra from their highest-symmetry orientation. We have adopted this method for analyzing the structure of the precipitate. The rotation axes of the octahedra are assumed to be the ⟨111⟩ directions of the cubic unit cell.

Fig. 4. indicates the arrangement of F ions around the Al ion at 0,0,0, which are displaced from the highest-symmetry positions as a result of the rotation of the AlF_6 octahedron by an angle ω around [111], where the initial orientation of the octahedron is represented by dashed lines. Then, the F ion at s,0,0 is displaced to sx, xy, sz, where

$$x = (1 + 2\cos\omega)/3$$
$$y = \sin\omega/3^{1/2} + (1 - \cos\omega)/3, \quad (4)$$
$$z = -\sin\omega/3^{1/2} + (1 - \cos\omega)/3.$$

The other F ions of the same octahedron are also displaced to new positions and their coordinates are obtained by interchanging the order of the coordinates x, y, z and by taking into account the sign of s. Then, the structure factor of the rotated octahedron is given by

$$f_{AlF_6} = f_{Al} + 2f_F[\cos 2\pi s(hx + ky + lz) + \cos 2\pi s(hz + kx + ly) + \cos 2\pi s(hy + kz + lx)]. \quad (5)$$

In order for the arrangement of the F ions to conform to the cubic symmetry, all eight ⟨111⟩ directions should be taken into account. Diffraction intensities are averages over all these possible modes of rotation. With the assumption that all the types of rotation of the AlF_6 octahedra are randomly distributed over the lattice points occupied by the octahedra,* the structure factor of one octahedron is expressed by a mean value of those corresponding to the eight possible modes of rotation. Thus, the structure factor of one AlF_6 octahedron is

$$f_{AlF_6} = f_{Al} + 2f_F\Phi, \quad (6)$$

where

$$\Phi = (\Phi_1 + \Phi_2 + \Phi_3 + \Phi_4 + \Phi_5 + \Phi_6 + \Phi_7 + \Phi_8)/8 \quad (7)$$

* This expression for the mode of distribution of the rotation axes is not strictly correct. More detailed considerations are given in § 5.

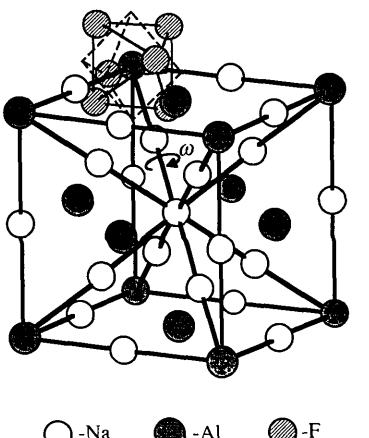

Fig. 4. Diagram representing the arrangement of F ions as a result of the rotation of the AlF_6 octahedron around the [111] axis by an angle ω. The initial orientation of the octahedron is represented by dashed lines.

and

$$\Phi_1 = \cos 2\pi s(hx + ky + lz) + \cos 2\pi s(hz + kx + ly) + \cos 2\pi s(hy + kz + lx),$$

$$\Phi_2 = \cos 2\pi s(-hx + ky + lz) + \cos 2\pi s(-hz + kx + ly) + \cos 2\pi s(-hy + kz + lx),$$

$$\Phi_3 = \cos 2\pi s(hx - ky + lz) + \cos 2\pi s(hz - kx + ly) + \cos 2\pi s(hy - kz + lx),$$

$$\Phi_4 = \cos 2\pi s(-hx - ky + lz) + \cos 2\pi s(-hz - kx + ly) + \cos 2\pi s(-hy - kz + lx), \quad (8)$$

$$\Phi_5 = \cos 2\pi s(hx + kz + ly) + \cos 2\pi s(hy + kx + lz) + \cos 2\pi s(hz + ky + lx),$$

$$\Phi_6 = \cos 2\pi s(-hx + kz + ly) + \cos 2\pi s(-hy + kx + lz) + \cos 2\pi s(-hz + ky + lx),$$

$$\Phi_7 = \cos 2\pi s(hx - kz + ly) + \cos 2\pi s(hy - kx + lz) + \cos 2\pi s(hz - ky + lx),$$

$$\Phi_8 = \cos 2\pi s(-hx - kz + ly) + \cos 2\pi s(-hy - kx + lz) + \cos 2\pi s(-hz - ky + lx),$$

corresponding to the eight possible ⟨111⟩ directions of the rotation axes. The structure factor of the unit cell is obtained from (1) by using (6), (7) and (8). Then, the relative intensities are given by (3).

Fig. 5 shows $I/I(0)$ as a function of the rotation angle ω calculated for different values of u. The overall features of the curves change rather drastically with u. However, they have common features. They are symmetric at $\omega = \pi/3$ rad and are cyclic with a period $2\pi/3$ rad because of the threefold symmetry around the ⟨111⟩ directions. While some of the reflections, such as the 200 and 222 reflections, change with both u and ω very sensitively, other reflections, such as 111 and 220 reflections, are almost invariant. At $\omega = 0$, which corresponds to the highest-symmetry orientation of the AlF_6 octahedra, the 222 reflection is very strong, while the 311 reflection is very weak, contrary to observation. With increasing ω, the 311 reflection increases while the 222 reflection decreases remarkably, to a deep minimum. These facts suggest that the characteristics of the diffraction intensities of the precipitate can be explained by taking into account the rotation of the octahedra.

Qualitative comparisons of these curves to the observed intensities have been made. In the case of Fig. 5(*a*), which corresponds to $u = 1/63$, the ω dependence of the 222 reflection is nearly the same as that of the 200 reflection and this case does not

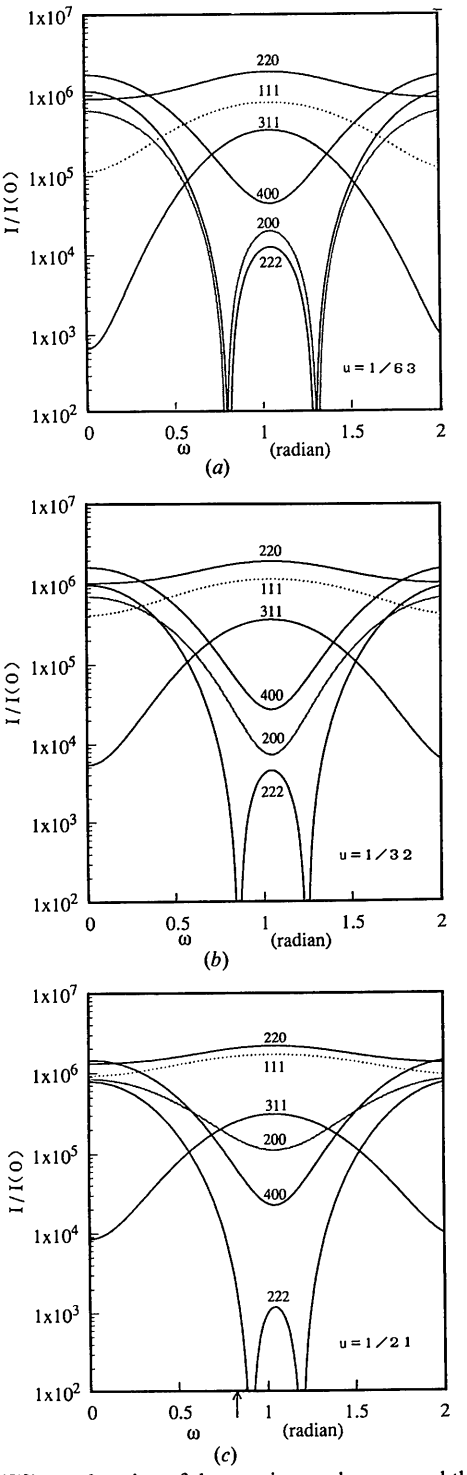

Fig. 5. $I/I(0)$ as a function of the rotation angle ω around the ⟨111⟩ axes, which are calculated by averaging structure amplitudes. (*a*) $u = 1/63$. (*b*) $u = 1/32$. (*c*) $u = 1/21$.

represent the observed features. In the case of Fig. 5(*b*), which corresponds to $u = 1/32$, the 200 reflection becomes larger than the 222 reflection but is insufficient to explain the observed intensities. In the case of Fig. 5(*c*), which corresponds to $u = 1/21$, fairly good agreement can be attained at $\omega \simeq 0.82$ rad (47°) indicated by an arrow in Fig. 5(*c*). Also, reflections with other indices also show good agreement between observed intensities and $I/I(0)$ at $\omega \simeq 0.82$ rad in Fig. 5(*c*).

5. Results and discussions

We have found that the mixed crystals of NaF doped with 1 mol% AlF_3 contain precipitates that are incoherent to the matrix lattice. However, the phase diagram shown in Fig. 1 indicates that the present system exhibits solid solubility up to a few mol% AlF_3, contrary to our observation. We think that this phase diagram is incorrect in the region of low AlF_3 concentration. We have recently become aware of another phase diagram for the same system, which indicates a eutectic phase for even very low concentrations of AlF_3 (Puschin & Baskow, 1913). This phase diagram agrees with our observation.

The chemical compositions of the precipitates have not been measured but the structure of the precipitate has been investigated in the framework of X-ray diffraction. The importance of checking chemical composition is emphasized by Steward (1992).

Almost all the diffraction lines of the precipitates in NaF doped with AlF_3 are indexed by the f.c.c. structure with lattice parameter 7.77 Å at room temperature. The volume of the cubic cell of the precipitates is equal to that of the pseudocubic cell of cryolite. These facts suggest that the structure is analogous to that of cubic Na_3AlF_6.

The diffraction intensities of the precipitate are characterized by very strong 311 and extremely weak 222 reflections. In order to explain these features, various kinds of modifications of the cubic Na_3AlF_6 structure were examined as a first step of the investigation: for example, some of the Na ions at body centers of the sublattice may be transferred to neighboring face-centered sites; Na ions at body centers of the sublattice may be displaced along body diagonals of the sublattice, analogous to the pyrite structure. However, the intensities of the 311 and 222 reflections could not be explained without the rotation of the octahedra being taken into account.

Because each octahedron is composed of a number of ions, its volume is large and its symmetry is nonspherical. Moreover, the octahedra will be rotated in a confined space of the unit cell so the displaced F ions of the rotated octahedron may have an effect on the rotation of the octahedra at nearest-neighbor positions. As a result, all the octahedra in one unit cell should have the same type of rotation.

We can consider different kinds of distribution of the rotation axes, depending on the size of the region, called a domain, in which one type of rotation takes place. The domains corresponding to different types of rotation are randomly distributed over the precipitates. Corresponding to the different sizes of the domains, two types of average are possible: (i) The sizes of the domains are small compared with that of the coherent region,* and all the types of the domains are randomly distributed in the interior of the coherent region. In this case, diffraction intensities are obtained by averaging structure amplitudes. The model of random distribution over the lattice points as described in § 4 corresponds to the extremity of this case. (ii) The sizes of the domains are relatively large and every coherent region is composed of one type of domain. In this case, intensities are obtained by averaging squares of structure amplitudes. It is clear from inspections of the lattice symmetry that the latter case does not correspond to the precipitates. We have further confirmed that the calculated intensities for the latter case do not explain the observation.

In the case of rotation around the ⟨111⟩ directions, the analysis is relatively simple because all six F ions around each Al ion are displaced by the same amount. There remain other possibilities such as ⟨100⟩ and ⟨110⟩ and some other directions for the rotation axes of the octahedra. It is necessary to ascertain whether the structure model is improved. The origin of the 210 and 230 reflections is not clear. The final goal of the present investigation is to arrive at a model that can explain completely all the reflections, including 210 and 230. Modification of the cubic Na_3AlF_6 structure into a pyrite-like structure and/or nonuniform distribution of the rotation axes of the octahedra may represent possible solutions to these problems.

The author expresses his sincere thanks to Professor E. G. Steward for permission to use his data and for the offer of valuable information and advice. Further, he expresses his hearty thanks to Professor H. Adachi of the Muroran Institute of Technology for valuable advice and support in the experimental work and to Professors Y. Shiozaki and K. Hayakawa of Hokkaido University for stimulating discussions.

* The term 'coherent region' implies a region of the crystal lattice in which the amplitudes of the scattered X-rays are additive and can therefore produce interference. The size of the coherent region is assumed to be smaller than that of the precipitates.

References

FEDOTIEFF, P. P. & ILJINSKII, W. P. (1913). *Z. Anorg. Chem.* **80**, 113–154.
HUHEEY, J. E. (1983). *Inorganic Chemistry*. New York: Harper & Row.
MAJUMDAR, A. J. & ROY, R (1965). *J. Inorg. Nucl. Chem.* **27**, 1961–1973.
MIYAKE, S. & SUZUKI, K. (1954*a*). *Acta Cryst.* **7**, 514–515.
MIYAKE, S. & SUZUKI, K. (1954*b*). *J. Phys. Soc. Jpn*, **9**, 702–712.
NARAY-SZABO, ST. V. & SASVARI, K. (1938). *Z. Kristallogr.* **99**, 27–31.
PUSCHIN, N. & BASKOW, A. (1913). *Z. Anorg. Chem.* **81**, 347–363.
STEWARD, E. G. (1992). Personal communication.
STEWARD, E. G. & ROOKSBY, H. P. (1953). *Acta Cryst.* **6**, 49–52.
SUZUKI, K. (1955). *J. Phys. Soc. Jpn*, **10**, 794–804.
SUZUKI, K. (1958). *J. Phys. Soc. Jpn*, **13**, 179–186.
SUZUKI, K. (1961). *J. Phys. Soc. Jpn*, **16**, 67–78.

Acta Cryst. (1993). A**49**, 853–866

Holographic Methods in X-ray Crystallography. II. Detailed Theory and Connection to Other Methods of Crystallography

BY ABRAHAM SZÖKE*

Lawrence Livermore National Laboratory, Livermore, CA 94550, USA

(*Received* 11 *November* 1992; *accepted* 21 *April* 1993)

Abstract

Equations are derived for finding an unknown part of the electron density in the unit cell of a crystal when part of the structure of its contents is already known. These equations are based on the similarity of the X-ray diffraction pattern to a hologram. The X-ray field scattered by the known part of the structure is identified as the holographic reference beam. It interferes with the waves scattered from the unknown part of the structure. The interference pattern contains phase information that can be exploited to recover fully the unknown part of the structure. This paper discusses mathematical properties of the resulting equations and some methods for their solution. A strong similarity to inverse problems of image processing is pointed out and connections to other known methods of X-ray crystallography are established. In paper III [Maalouf, Hoch, Stern, Szöke & Szöke (1993). *Acta Cryst.* A**49**, 866–871], some modest numerical simulations are presented.

Introduction

A basic ingredient of crystallographic refinement is the recovery of an unknown part of a crystal structure from its diffraction pattern when part of the structure is already known at least approximately. The traditional methods of doing this are widely known and practised by crystallographers. This paper presents an alternative method based on the similarity of X-ray diffraction to holography. The X-ray field scattered by the known part of the structure is identified as the holographic reference beam. It interferes with the waves scattered from the unknown part of the structure. The diffraction pattern detected is analogous to the recorded hologram. As in holography, the X-ray diffraction spots are considered as a pattern and not individually. Recovery of the unknown part is then shown to be a result of the solution of a set of equations. The roots of the point of view expressed in this paper go back at least to Bragg (1939, 1942, 1944) and to Boersch (1939), whose papers were the very articles that inspired Gábor's discovery of holography (Gábor, 1948, 1949). Early work was summarized in a book by Taylor & Lipson (1964). Recently, this line of inquiry has apparently not been pursued, although somewhat related ideas have been presented by Bricogne (1988) and Doerschuk (1991). Some of these ideas were briefly presented by the author in paper I (Szöke, 1992).

The present approach has several potentially attractive features. The unknowns in the holographic equations are the electron density in real space; therefore, it is relatively easy to incorporate additional information into the solution of the structure. It is shown that, by forcing the electron density to be positive, the stability of the recovery of the unknown part is improved. Because this ensures the positivity of all the Karle–Hauptman determinants, as well as the correct behavior of all structure invariants and semi-invariants, the holographic method incorporates part of the information utilized in direct methods. It is also shown that the missing part of the molecule is recovered, theoretically, to better accuracy by this method than by the difference Fourier method. In particular, the known part of the structure does not introduce a first-order phase bias into the resulting electron-density map. The solution of the holographic equations is somewhat similar to a Fourier recovery of the unknown part, with constraints enforced during the recovery, or to the completion of a crystal structure si-

* This work was performed under the auspices of the US Department of Energy, under contract no. W-7405-ENG-48.

©1993 International Union of Crystallography
Printed in Great Britain – all rights reserved